THE JOURNAL OF PHYSICAL CHEMISTRY Letters

pubs.acs.org/JPCL Letter

Whispering-Gallery Mode Lasing in Perovskite Nanocrystals Chemically Bound to Silicon Dioxide Microspheres

Michael B. Price,* Keiran Lewellen, Jake Hardy, Stephanie M. Lockwood, Chase Zemke-Smith, Isabella Wagner, Meiqi Gao, Johan Grand, Kai Chen, Justin M. Hodgkiss, Eric Le Ru, and Nathaniel J. L. K. Davis*

Cite This: J. Phys. Chem. Lett. 2020, 11, 7009−7014 Read Online

ACCESS | Metrics & More | Article Recommendations | Supporting Information

ABSTRACT: Cesium lead halide perovskite nanocrystals exhibit high photoluminescence quantum efficiencies and tunability across the visible spectrum. This makes these crystals ideal candidates for solar panels, light-emitting diodes, lasers, and especially nanolasers. Due to the versatility of cation substitution in perovskite nanocrystals, they can be grown on amine-functionalized silicon dioxide nanoparticles, where the amine linker replaces the standard cation structure. Selectively growing luminescent nanocrystals on spherical silicon dioxide microspheres results in the opportunity to populate whispering-gallery modes in these spherical silica microspheres. In this case, the nanocrystal halide composition can be used to selectively tune the emission wavelength mode, and microsphere radius to tune the mode spacing. This silicon dioxide attachment also adds to the overall stability of the system. Through photoluminescence microscopy measurements, we show whispering gallery modes in individual perovskite-coated microspheres for $CsPbBr_3$ and $CsPbI_3$ nanocrystals on 9.2 μm diameter silica spheres and compare these to theoretically predicted optical modes. In $CsPbBr_3$, we provide evidence that these modes will lase under optical excitation, with a threshold of 750 $\mu J/cm^2$. This study presents a novel system that, through optimization, could be a promising pathway to achieve facile and stable perovskite nanolasers.

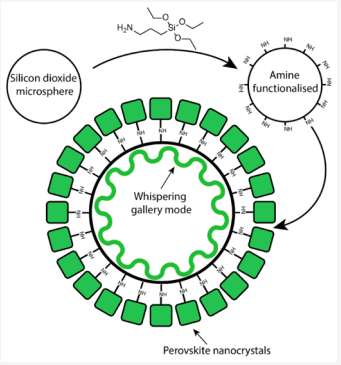

Nanolasers are important for the use of optoelectronic integrated circuit technologies, due to their easily tunable wavelengths, affordability, size, and high power efficiencies compared with conventional lasers. Cesium lead halide perovskite nanocrystals (NCs) exhibit high photoluminescence quantum efficiencies (PLQEs), approaching 100%, making these crystals ideal candidates for lasers, solar panels, and light-emitting diodes (LEDs).[1−3]

Properties that make perovskite NCs well-suited for lasing applications also include low-cost precursor materials and facile synthesis, highly efficient and narrow-band emission, and broad absorption spectra with high absorption coefficients.[4−6] Since bulk perovskite's first demonstration of amplified spontaneous emission (ASE)[7] and vertical cavity lasing,[8] they have been tailored to a wide variety of nanolasing configurations,[1,3,9−14] with impressively low optical excitation thresholds. However, research is ongoing in the quest to achieve electronically pumped lasing.[15]

Due to their high thermal stability (400−500 °C compared with 150 °C for organometallic perovskite NCs[11]) inorganic perovskite NCs are preferable for use in lasers, where the requirement for high excited state densities necessitates thermal stability. However, perovskite NC surface ligands, and surfaces, are easily damaged by polar solvents; therefore, their stability is still an ongoing issue.[4] In particular, water reacts readily with perovskite NCs, limiting their applications.[16] Recent results present a way of enhancing the water stability and longevity of cesium lead halide perovskite NCs by growing them on amine-functionalized silica (SiO_2) nanowires.[17]

We extend this concept by chemically coupling perovskite NCs to silicon dioxide microspheres. The silica microspheres are aminated by (3-aminopropyl)triethoxysilane and added to the standard hot injection synthesis method of cesium perovskite NCs[18] to effectively grow the perovskite NCs on the surfaces of the silica microsphere (Figure 1). In previous studies, involving SiO_2 nanowires, the suppression of moisture intolerance was observed for up to 60 days.[17] We have observed similar enhancements in stability.

The silica microspheres function as a cavity, where selective optical modes are enhanced by internal reflection into optical whispering-gallery modes (WGMs).[19] Whispering-gallery mode lasers are suitable for "laser on a chip" applications. They have high quality "Q" factors, enabling low lasing thresholds and highly selective modes, and they can be made

Received: June 29, 2020
Accepted: August 6, 2020
Published: August 6, 2020

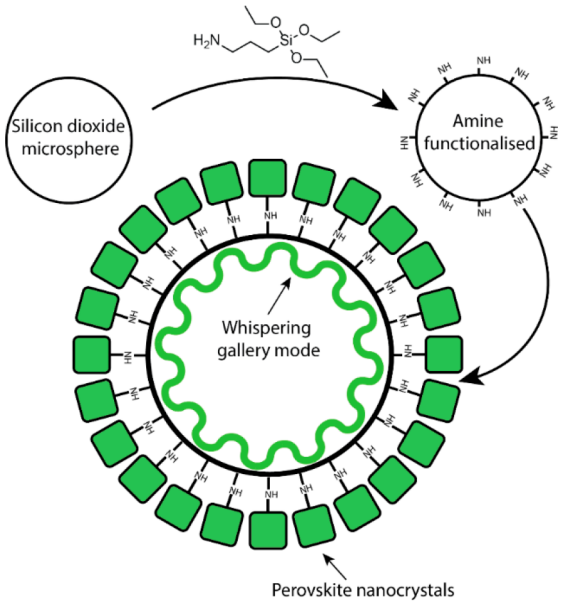

Figure 1. Scheme illustrating the concept of whispering-gallery mode emission into SiO_2 microspheres from chemically attached perovskite nanocrystals.

by simple fabrication procedures, as they have an intrinsic cavity and do not require the strict optical design and engineering of other traditional cavities. Perovskite whispering-gallery mode lasers have been made with a variety of nanoplatelet, and nanostructured shapes formed by pure perovskite materials,[1,9,20] or on templates.[21] Notably, very low lasing thresholds were achieved by sequential drop-casting of silica microspheres and then subsequent deposition of $CsPbX_3$ (X = Cl, Br, and I) nanoparticles.[11]

Here we present a novel method of achieving optically pumped microlasing through perovskite nanocrystals chemically attached to SiO_2 microspheres. We synthesize $CsPbBr_3$ and $CsPbI_3$ nanocrystals attached to 9.2 μm diameter SiO_2 spheres and characterize the photoluminescence properties of these functionalized microspheres. We show the presence of well-defined optical modes in single perovskite-functionalized microspheres through photoluminescence microscopy, correlate these modes to predictions based on Mie theory, and provide evidence of optically pumped lasing in a small ensemble of $CsPbBr_3$-functionalized microspheres, with a lasing threshold of 750 $\mu J/cm^2$.

This study presents a proof of principle for a new class of single-deposition-step lasing materials that offer many potential benefits compared to traditional nanolaser designs, including increased versatility, stability, and scope for decreasing lasing threshold through thermal management.

We first grow perovskite nanoparticles onto small SiO_2 nanoparticles, using a modified literature procedure,[5] to prove that particles do indeed grow as expected around the silica, as a first step. We initially use much smaller SiO_2 nanoparticles (~15 nm diameter) to remove any confounding waveguide effects in our absorption and photoluminescence characterisations. Briefly, we aminate silica dioxide nanoparticles via soaking the SiO_2 nanoparticles in a solution of (3-aminopropyl)trimethoxysilane in toluene for 24 h. These nanoparticles are then washed via centrifugation and redispersal in hexane. The perovskite nanocrystals are synthesized via a modified literature procedure[5] via the addition of 20 mg of the aminated silica nanoparticles to the reaction vessel. Finally, the perovskite/silica nanoparticles are washed via centrifugation and redispersal in hexane.

Figure 2a shows the normalized absorption and photoluminescence spectra of the synthesized nanocrystals on SiO_2, in solution. They show the characteristic narrow emission and

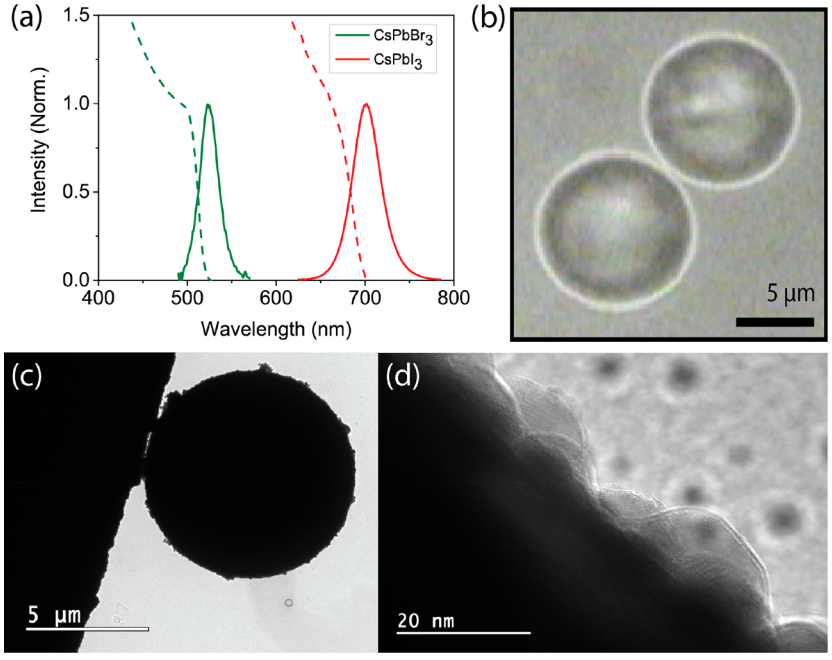

Figure 2. (a) Absorption (dashed) and emission (solid) of $CsPbBr_3$ and $CsPbI_3$ grown on SiO_2 nanoparticles. (b) Optical microscope image of $CsPbBr_3$ nanoparticle-functionalized SiO_2 microspheres on glass substrate. Low (c) and high resolution (d) TEM images of $CsPbBr_3$–SiO_2 micropatricles.

https://dx.doi.org/10.1021/acs.jpclett.0c02003
J. Phys. Chem. Lett. 2020, 11, 7009−7014

low Stokes shift optical spectra of cesium lead halide nanocrystals.[22] Supplementary Figures 1 and 2 also show the typical cubic structures of the nanocrystals under TEM.[22]

Having confirmed the efficacy of the nanocrystal synthesis procedure, and the successful attachment of the nanocrystals to SiO_2, we perform the same procedure with SiO_2 microspheres, of 1.5 and 9.2 μm average diameter, purchased from Cospheric. On the basis of Mie theory simulations detailed below, the 1.5 μm spheres would be expected to show single mode emission, but the relevant modes would be broad and relatively weak (see supplementary Figure 3). The 9.2 μm spheres were predicted to show much stronger and narrower modes, while still being spaced far enough apart in energy to be easily distinguished. Figure 2b shows an optical microscope image of the nanocrystal-functionalized 9.2 μm microspheres after 10 complete wash cycles and subsequent drop-casting onto a microscope slide. The two spheres shown are representative of the majority of the spheres observed, showing relatively uniform coverage of nanoparticle materials, although some spheres showed an interesting "ring-like" distribution of nanocrystal coverage (Supplementary Figure 4). These incompletely covered spheres did not show any discernible modes in their emission. Figure 2c,d show TEM images of the synthesized $CsPbBr_3$ nanocrystals on SiO_2 and Supplementary Figure 5 shows the elemental analysis that confirms attachment.

The green curve in Figure 3 shows the emission of a single NC-functionalized microsphere, pumped with 458 nm light

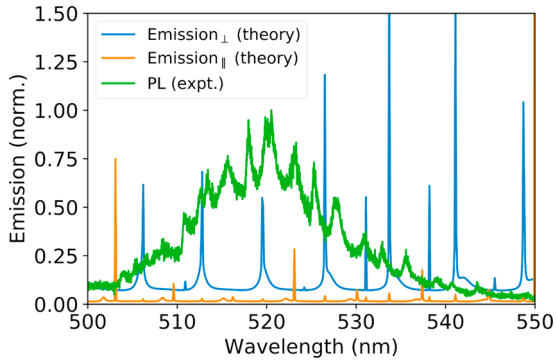

Figure 3. PL emission and modes (normalized) from a single perovskite-functionalized SiO_2 microsphere (green line). The whispering-gallery modes are clearly distinguishable and spaced approximately 12 meV apart. The blue and orange curves are the scaled radiative power of a dipole either perpendicular (blue) or parallel (orange) to the sphere located at a distance of 1 nm from the surface. These highlight the whispering-gallery modes that an emitter can couple to.

focused to a 2 μm spot size, and measured through an objective. The measured spectrum clearly shows well-defined and sharp whispering-gallery modes overlaid onto the standard $CsPbBr_3$ NC emission. The mode spacing in this wavelength region is 12 meV, which is consistent across other individual microspheres, but it is apparent that small differences in microsphere size or nanocrystal coverage give rise to differences in mode position and prominence (see Supplementary Figure 6), which leads to a "smearing out" of the multiple modes present, if viewed as an ensemble. Single microsphere PL measurements also showed that it was possible to observe whispering-gallery modes in $CsPbI_3$-functionalized spheres (Supplementary Figure 7), although these modes were less well-defined, these iodide NCs were less stable than their bromide counterparts, and these iodide-attached spheres did not ultimately exhibit any lasing characteristics.

To aid in our initial design, and complement our experimental measurements, we simulated the light scattering caused by dipole emission from the edge of a SiO_2 microsphere. The simulation was performed using a generalization of Mie theory to calculate the radiation properties of a dipolar emitter next to a sphere or a spherical multilayer.[23,24] The blue and orange lines in Figure 3 represent the emission modes as evidenced through the calculated radiated power (scaled) from a dipole source arranged perpendicular and parallel to the sphere, respectively. While the real measured modes will be subject to broadening (from both homogeneous and inhomogeneous broadening mechanisms, and variations in microsphere shape and nanocrystal coverage), the mode spacing between the simulated modes, of ~15 meV, is in reasonable agreement with the average measured mode spacing (12 meV) for the 9.2 μm spheres.

As final proof of the potential of this method of chemical functionalization to be useful in real world devices, we show that lasing is possible from an ensemble of spheres. We measured the light emission from small ensembles of microspheres (estimated to be between 3 and 10 spheres in Figure 4), dropcast onto a glass substrate, pumped by a 150 fs, 400 nm laser pulse of increasing incident intensity, and measured by an intensified charge coupled device (iCCD). Figure 4a presents the emission spectra as the fluence was increased, showing the clear appearance of a sharp emission mode at 527 nm above a threshold of 750 μJ/cm^2. We fit the PL peak, and 527 nm peak with Lorentzian functions, and plot

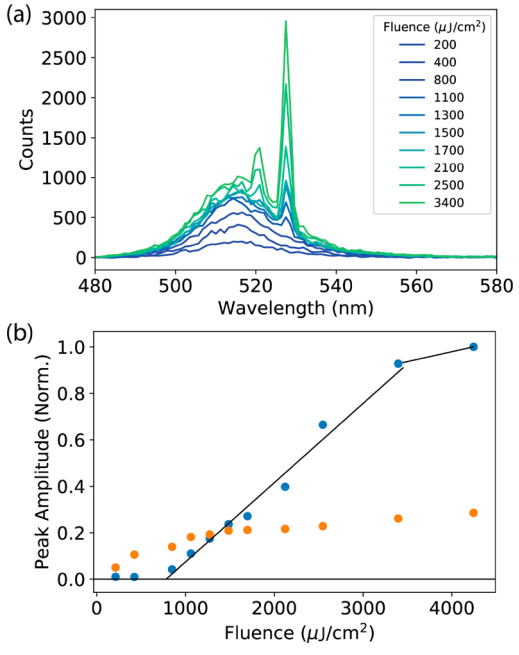

Figure 4. (a) Fluence dependent emission spectra of drop-cast NC-coated SiO_2 microspheres. Two fluence-dependent, sharp modes appear beyond an incident fluence of 750 μJ/cm^2, 400 nm pulsed excitation. (b) Fitted peak amplitudes comparing the PL baseline peak (orange circles) to the fitted main modal peak at 527 nm (blue circles). The black lines are linear fits to the data to guide the eye. The "S-shape" of the blue peak amplitude, in contrast to the orange PL amplitude, evidence optically pumped lasing.

https://dx.doi.org/10.1021/acs.jpclett.0c02003
J. Phys. Chem. Lett. 2020, 11, 7009−7014

their amplitudes (normalized) in Figure 4b. While the main PL peak, centered at 517 nm, follows a sublinear amplitude dependence, the 527 nm lasing peak exhibits the requisite "s-like" curve of optically pumped lasing. We consider that the system is lasing, rather than undergoing amplified spontaneous emission (ASE) within the whispering-gallery modes, due to four key considerations: (1) The mode does not broaden with increasing pump power, as seen in other very similar systems undergoing ASE.[11] (2) No ASE was observed under any given fluence for systems that did not exhibit these peaks, for instance, in the 1.5 μm spheres coated with the same nanocrystals. (3) The mode is narrow (fwhm ∼2 nm), even for an ensemble of microspheres. (4) The very characteristic s-shaped curve seen in Figure 4b. We estimate a rough cavity Q-factor of ∼210 from the ensemble of spheres, based on the fwhm of the spectral peak just above the lasing threshold.[25]

The thermal stability of this system is promising. Under a nitrogen atmosphere, lasing modes still appear unchanged at moderate fluences, even after 10 min of exposure to extremely high incident pump intensities (fluences over 4 mJ/cm^2). Efficient PL, with no intensity droop, was also observed in air over many hours, although without exposure to extreme fluences. This shows photostability similar in level to other reports in literature.[1,26] To further investigate the thermal stability, we measured the luminescent intensity as a function of applied temperature for both attached and unattached nanocrystals in air. We find that the as synthesized $CsPbBr_3$ nanocrystals begin to degrade at ∼100 °C in air while the nanocrystals attached to SiO_2 nanocrystal maintain their luminescence intensity until 140 °C (Supplementary Figure 8). This is likely due to the increased thermal conduction afforded by the intimate contact of the perovskite with the silica, and the increased chemical stability due to the ligands bound to both the perovskite and the silica.

While the threshold for the onset of lasing is high in comparison to some other perovskite microlaser systems, the successful demonstration of lasing illustrates our approach's potential, given its advantages in stability[17] and ease of processing. There is much scope to decrease the lasing threshold in this system to the low levels measured in other systems: principally by increasing the photoluminescence quantum efficiency of the functionalized nanocrystals, by optimization of their synthesis with focus on the ligand effects, and also by decreasing the polydispersity of the microsphere scaffolds and increasing their size and refractive indices for more defined whispering-gallery modes. By chemically attaching the NCs to the spheres, instead of depositing through other means such as spin-coating or vapor depositing, there are substantial practical advantages that can be gained, such as easy one-step coating onto existing light sources, better conformal coating, and better environmental and thermal stability.

We have demonstrated optically pumped lasing at room temperature from $CsPbBr_3$ nanocrystals chemically attached to SiO_2 microspheres. We have attached $CsPbBr_3$ and $CsPbI_3$ NCs to SiO_2 microspheres of different sizes by a simple modified nanocrystal synthesis procedure and observed optical whispering-gallery modes for both nanocrystal species with the larger microsphere resonator scaffolds. This work lays the pathway for future optimization of this versatile system. With further threshold optimization, the benefits of a one-step deposition solution-processable nanolaser may be realized in future devices, offering the potential for cheaper and more versatile fabrication and improved thermal management.

EXPERIMENTAL METHODS

All chemicals were purchased from Sigma-Aldrich and used as received.

Simulations. Simulations were performed with existing Matlab code package SPlaC.[23,24] The simulations are based on a generalization of Mie theory to dipolar emitters near a sphere or sphere multilayer. The radiated power can be calculated as a function of wavelength to highlight modes that an emitter can efficiently couple to. The refractive index of SiO_2 was taken from www.refractiveindex.info[27] and the embedding medium was assumed to be air (as in the experiments).

Aminated Silica Nanospheres. Microspheres of 9.2 and 1.5 μm were purchased from Cospheric incorporated. A solution of (3-aminopropyl)trimethoxysilane (APTES, 5% wt) was made by diluting 0.4 mL APTES in 7.6 mL of toluene and adding 169 mg of 9.2 μm silica (SiO_2) microspheres, this solution was left for 24 h in a capped 20 mL sample vial with vigorous stirring. These nanoparticles were washed via centrifugation and redispersal in hexane.

Nanocrystal Synthesis. The nanocrystals were synthesized via a modified literature procedure[5] as detailed below. Cesium oleate was prepared via the addition of Cs_2CO_3 (0.814 g) into a 100 mL three-neck with a stir bar along with octadecyl (ODE, 40 mL) and OA (2.5 mL). This mixture was then dried for 1 h at 120 °C under vacuum.

Separately PbX_2 (X = Br, I) (0.188 mmol), ODE (5 mL), OA (0.5 mL), oleylamine (OLAM, 0.5 mL) and 20 mg of the aminated silica particles were added into a 25 mL 3-necked round-bottom flask with a stir bar. The mixture was dried under nitrogen for 1 h at 120°C. After drying the solutions were flushed with nitrogen and heated to 170°C.

Two milliliters of cesium oleate was injected into the PbX_2 solution at 170 °C. The reaction was quenched in an ice−water bath approximately 5 s after the injection. The perovskite/silica particles were collected and purified by centrifugation (1500 rpm for 2 min) and redispersion in anhydrous hexane. Nine wash cycles were used to ensure only NCs attached to silica remained.

Fluorometer Measurements. Nonattached nanocrystals (separate from microspheres) in solution were measured in a quartz glass cuvette and diluted with anhydrous hexane. Steady-state solution fluorescence measurements were carried out on an Edinburgh Photonics FLS-980 spectrophotometer with a 450W ozone-free xenon arc lamp.

Microscope Photoluminescence Measurements and Optical Microscope Images. Single microsphere fluorescence was carried out with a Jobin-Yvon Labram HR spectrometer, equipped with a liquid Nitrogen cooled CCD detector, in the backscattering configuration through a microscope objective (A ×100 Olympus air objective, NA 0.9) The samples were excited with a 514 nm argon-ion laser and filters were used to reduce the power as needed. Optical images were taken on the same setup but in transmission configuration, and recorded on a digital camera. Nanocrystal-coated microspheres were drop-cast onto a microscope slide at sufficiently dilute concentrations to ensure individual microspheres could be resolved and not touch other microspheres. These dropcast spheres were measured in air.

https://dx.doi.org/10.1021/acs.jpclett.0c02003
J. Phys. Chem. Lett. 2020, 11, 7009−7014

Lasing Measurements. Microspheres were drop-coated onto a spectrosil substrate and encapsulated in nitrogen and were pumped with a 400 nm excitation beam, focused to a spot-size 70 μm in diameter. The pump was generated from a Ti:sapphire amplifier system (Spitfire Ace) operating at 3kH and generating 150 fs pulses at 800 nm converted to 400 nm using an optical parametric amplifier (TOPAS, Light Conversion). The scatter of the excitation beam was suppressed using a 435 nm long-pass filter and the emitted light was focused onto a spectrometer and iCCD.

TEM Analysis. TEM pictures were recorded on a JEOL JEM-2100F FE field emission electron microscope under 200 kV acceleration. EDS maps were performed looking for the elements C, O, Si, Cs, Pb, and Br.

■ ASSOCIATED CONTENT

Supporting Information

The Supporting Information is available free of charge at https://pubs.acs.org/doi/10.1021/acs.jpclett.0c02003.

TEM images, simulated scattering modes, optical microscopy image, elemental analysis maps, emission spectra, whispering gallery mode emission spectra, and thermal degradation graph (PDF)

■ AUTHOR INFORMATION

Corresponding Authors

Michael B. Price − *School of Chemical and Physical Sciences and The MacDiarmid Institute for Advanced Materials and Nanotechnology, Victoria University of Wellington, Wellington 6140, New Zealand; The Dodd-Walls Centre for Photonic and Quantum Technologies, University of Otago, Dunedin 9056, New Zealand*; Email: michael.price@vuw.ac.nz

Nathaniel J. L. K. Davis − *School of Chemical and Physical Sciences and The MacDiarmid Institute for Advanced Materials and Nanotechnology, Victoria University of Wellington, Wellington 6140, New Zealand; The Dodd-Walls Centre for Photonic and Quantum Technologies, University of Otago, Dunedin 9056, New Zealand;* orcid.org/0000-0003-2535-8968; Email: nathaniel.davis@vuw.ac.nz

Authors

Keiran Lewellen − *School of Chemical and Physical Sciences, Victoria University of Wellington, Wellington 6140, New Zealand*

Jake Hardy − *School of Chemical and Physical Sciences, Victoria University of Wellington, Wellington 6140, New Zealand*

Stephanie M. Lockwood − *School of Chemical and Physical Sciences, Victoria University of Wellington, Wellington 6140, New Zealand*

Chase Zemke-Smith − *School of Chemical and Physical Sciences, Victoria University of Wellington, Wellington 6140, New Zealand*

Isabella Wagner − *School of Chemical and Physical Sciences, Victoria University of Wellington, Wellington 6140, New Zealand*

Meiqi Gao − *School of Chemical and Physical Sciences, Victoria University of Wellington, Wellington 6140, New Zealand*

Johan Grand − *School of Chemical and Physical Sciences and The MacDiarmid Institute for Advanced Materials and Nanotechnology, Victoria University of Wellington, Wellington 6140, New Zealand; Université de Paris, F-75006 Paris, France*

Kai Chen − *School of Chemical and Physical Sciences and The MacDiarmid Institute for Advanced Materials and Nanotechnology, Victoria University of Wellington, Wellington 6140, New Zealand; The Dodd-Walls Centre for Photonic and Quantum Technologies, University of Otago, Dunedin 9056, New Zealand*

Justin M. Hodgkiss − *School of Chemical and Physical Sciences and The MacDiarmid Institute for Advanced Materials and Nanotechnology, Victoria University of Wellington, Wellington 6140, New Zealand;* orcid.org/0000-0002-9629-8213

Eric Le Ru − *School of Chemical and Physical Sciences and The MacDiarmid Institute for Advanced Materials and Nanotechnology, Victoria University of Wellington, Wellington 6140, New Zealand;* orcid.org/0000-0002-3052-9947

Complete contact information is available at: https://pubs.acs.org/10.1021/acs.jpclett.0c02003

Notes

The authors declare no competing financial interest.

■ ACKNOWLEDGMENTS

M.B.P. thanks the Royal Society of New Zealand for Rutherford Postdoctoral Fellowship funding. N.J.L.K.D. acknowledges research funding from the Victoria Research Trust, the Science for Technological Innovation Science Challenges, the Marsden Fund and the Ministry of Business, Innovation and Employment.

■ REFERENCES

(1) Tang, B.; Dong, H.; Sun, L.; Zheng, W.; Wang, Q.; Sun, F.; Jiang, X.; Pan, A.; Zhang, L. Single-Mode Lasers Based on Cesium Lead Halide Perovskite Submicron Spheres. *ACS Nano* **2017**, *11* (11), 10681−10688.

(2) Schubert, E. F.; Kim, J. K. Solid-State Light Sources Getting Smart. *Science (Washington, DC, U. S.)* **2005**, *308* (5726), 1274−1278.

(3) Sutherland, B. R.; Hoogland, S.; Adachi, M. M.; Wong, C. T. O.; Sargent, E. H. Conformal Organohalide Perovskites Enable Lasing on Spherical Resonators. *ACS Nano* **2014**, *8* (10), 10947−10952.

(4) Yang, Tonghui; Zhang, Zhe; Ding, Yanli; Yin, Naiqiang; Liu, X. Nondestructive Purification Process of Inorganic Perovskite Quantum Dot Solar Cells. *J. Nanopart. Res.* **2019**, *21*, 101.

(5) Protesescu, L.; Yakunin, S.; Bodnarchuk, M. I.; Krieg, F.; Caputo, R.; Hendon, C. H.; Yang, R. X.; Walsh, A.; Kovalenko, M. V. Nanocrystals of Cesium Lead Halide Perovskites (CsPbX3, X = Cl, Br, and I): Novel Optoelectronic Materials Showing Bright Emission with Wide Color Gamut. *Nano Lett.* **2015**, *15* (6), 3692−3696.

(6) Huang, H.; Bodnarchuk, M. I.; Kershaw, S. V.; Kovalenko, M. V.; Rogach, A. L. Lead Halide Perovskite Nanocrystals in the Research Spotlight: Stability and Defect Tolerance. *ACS Energy Lett.* **2017**, *2*, 2071−2083.

(7) Xing, G.; Mathews, N.; Lim, S. S.; Yantara, N.; Liu, X.; Sabba, D.; Grätzel, M.; Mhaisalkar, S.; Sum, T. C. Low-Temperature Solution-Processed Wavelength-Tunable Perovskites for Lasing. *Nat. Mater.* **2014**, *13*, 476.

(8) Deschler, F.; Price, M.; Pathak, S.; Klintberg, L. E.; Jarausch, D. D.; Higler, R.; Hüttner, S.; Leijtens, T.; Stranks, S. D.; Snaith, H. J.; Atatüre, M.; Phillips, R. T.; Friend, R. H. High Photoluminescence Efficiency and Optically Pumped Lasing in Solution-Processed Mixed Halide Perovskite Semiconductors. *J. Phys. Chem. Lett.* **2014**, *5* (8), 1421−1426.

(9) Zhang, Q.; Ha, S. T.; Liu, X.; Sum, T. C.; Xiong, Q. Room-Temperature near-Infrared High-Q Perovskite Whispering-Gallery Planar Nanolasers. *Nano Lett.* **2014**, *14* (10), 5995−6001.

(10) Zhang, Q.; Wang, R.; Hu, X.; Mi, Y.; Liu, X.; Shi, J.; Qiu, X.; Wu, Z.; Niu, X.; Chen, J.; Wu, T.; Du, W.; Liu, Z.; Shang, Q.; Zhang, S. Fabry-Pérot Oscillation and Room Temperature Lasing in

Perovskite Cube-Corner Pyramid Cavities. *Small* **2018**, *14* (9), 1703136.
(11) Yakunin, S.; Protesescu, L.; Krieg, F.; Bodnarchuk, M. I.; Nedelcu, G.; Humer, M.; De Luca, G.; Fiebig, M.; Heiss, W.; Kovalenko, M. V. Low-Threshold Amplified Spontaneous Emission and Lasing from Colloidal Nanocrystals of Caesium Lead Halide Perovskites. *Nat. Commun.* **2015**, *6*, 8056.
(12) Su, R.; Diederichs, C.; Wang, J.; Liew, T. C. H.; Zhao, J.; Liu, S.; Xu, W.; Chen, Z.; Xiong, Q. Room-Temperature Polariton Lasing in All-Inorganic Perovskite Nanoplatelets. *Nano Lett.* **2017**, *17* (6), 3982−3988.
(13) Zhu, H.; Fu, Y.; Meng, F.; Wu, X.; Gong, Z.; Ding, Q.; Gustafsson, M. V.; Trinh, M. T.; Jin, S.; Zhu, X.-Y. Lead Halide Perovskite Nanowire Lasers with Low Lasing Thresholds and High Quality Factors. *Nat. Mater.* **2015**, *14*, 636.
(14) Chen, S.; Roh, K.; Lee, J.; Chong, W. K.; Lu, Y.; Mathews, N.; Sum, T. C.; Nurmikko, A. A Photonic Crystal Laser from Solution Based Organo-Lead Iodide Perovskite Thin Films. *ACS Nano* **2016**, *10* (4), 3959−3967.
(15) Li, G.; Price, M.; Deschler, F.; Li, G.; Price, M.; Deschler, F. Research Update: Challenges for High-Efficiency Hybrid Lead-Halide Perovskite LEDs and the Path towards Electrically Pumped Lasing Research Update: Challenges for High-Efficiency Hybrid Lead-Halide Perovskite LEDs and the Path towards Electrically Pumpe. *APL Mater.* **2016**, *4*, 091507.
(16) Frost, J. M.; Butler, K. T.; Brivio, F.; Hendon, C. H.; van Schilfgaarde, M.; Walsh, A. Atomistic Origins of High-Performance in Hybrid Halide Perovskite Solar Cells. *Nano Lett.* **2014**, *14* (5), 2584−2590.
(17) Pan, A.; Jurow, M. J.; Wu, Y.; Jia, M.; Zheng, F.; Zhang, Y.; He, L.; Liu, Y. Highly Stable Luminous "Snakes" from $CsPbX_3$ Perovskite Nanocrystals Anchored on Amine-Coated Silica Nanowires. *ACS Appl. Nano Mater.* **2019**, *2* (1), 258−266.
(18) Protesescu, L.; Yakunin, S.; Bodnarchuk, M. I.; Krieg, F.; Caputo, R.; Hendon, C. H.; Yang, R. X.; Walsh, A.; Kovalenko, M. V. Nanocrystals of Cesium Lead Halide Perovskites (CsPbX(3), X = Cl, Br, and I): Novel Optoelectronic Materials Showing Bright Emission with Wide Color Gamut. *Nano Lett.* **2015**, *15* (6), 3692−3696.
(19) He, L.; Ozdemir, S. K.; Yang, L. Whispering Gallery Microcavity Lasers. *Laser Photon. Rev.* **2013**, *7*, 60.
(20) Liu, X.; Ha, S. T.; Zhang, Q.; De La Mata, M.; Magen, C.; Arbiol, J.; Sum, T. C.; Xiong, Q. Whispering Gallery Mode Lasing from Hexagonal Shaped Layered Lead Iodide Crystals. *ACS Nano* **2015**, *9*, 687.
(21) Sutherland, B. R.; Hoogland, S.; Adachi, M. M.; Wong, C. T. O.; Sargent, E. H. Conformal Organohalide Perovskites Enable Lasing on Spherical Resonators. *ACS Nano* **2014**, *8* (10), 10947−10952.
(22) Nedelcu, G.; Protesescu, L.; Yakunin, S.; Bodnarchuk, M. I.; Grotevent, M.; Kovalenko, M. V. Fast Anion-Exchange in Highly Luminescent Nanocrystals of Cesium Lead Halide Perovskites (CsPbX3, X = Cl, Br, I). *Nano Lett.* **2015**, *15* (8), 5635−5640.
(23) Le Ru, E. C.; Etchegoin, P. G. *Surface Enhanced Raman Spectroscopy and Related Plasmonic Effects*; Elsevier: Amsterdam, 2009.
(24) Le Ru, E. C.; Etchegoin, P. G. SERS and Plasmonics Codes (SPlaC), Matlab codes freely available from http://www.vuw.ac.nz/raman/book/codes.aspx.
(25) Liu, Y.; Fang, H.; Rasmita, A.; Zhou, Y.; Li, J.; Yu, T.; Xiong, Q.; Zheludev, N.; Liu, J.; Gao, W. Room Temperature Nanocavity Laser with Interlayer Excitons in 2D Heterostructures. *Sci. Adv.* **2019**, *5* (4), eaav4506.
(26) Liu, Z.; Yang, J.; Du, J.; Hu, Z.; Shi, T.; Zhang, Z.; Liu, Y.; Tang, X.; Leng, Y.; Li, R. Robust Subwavelength Single-Mode Perovskite Nanocuboid Laser. *ACS Nano* **2018**, *12* (6), 5923−5931.
(27) Refractive Index information, https://refractiveindex.info/ (accessed Jun 20, 2020).

https://dx.doi.org/10.1021/acs.jpclett.0c02003
J. Phys. Chem. Lett. 2020, 11, 7009−7014

Supplementary Information for:

Whispering-Gallery Mode Lasing in Perovskite Nanocrystals Chemically Bound to Silicon Dioxide Microspheres.

Michael B. Price[a,b,c]*, Keiran Lewellen[a], Jake Hardy[a], Stephanie M. Lockwood[a], Chase Zemke-Smith[a], Isabella Wagner[a], Meiqi Gao[a], Johan Grand[a,b,d], Kai Chen[a,b,c], Justin M. Hodgkiss[a,b], Eric C. Le Ru[a,b], and Nathaniel J. L. K. Davis[a,b,c]*

[a] School of Chemical and Physical Sciences, Victoria University of Wellington, Wellington 6140, New Zealand

[b] The MacDiarmid Institute for Advanced Materials and Nanotechnology, Victoria University of Wellington, Wellington 6140, New Zealand

[c] The Dodd-Walls Centre for Photonic and Quantum Technologies, University of Otago, Dunedin 9056, New Zealand

[d] Université de Paris, ITODYS, CNRS, F-75006 Paris, France

* Email: nathaniel.davis@vuw.ac.nz, michael.price@vuw.ac.nz

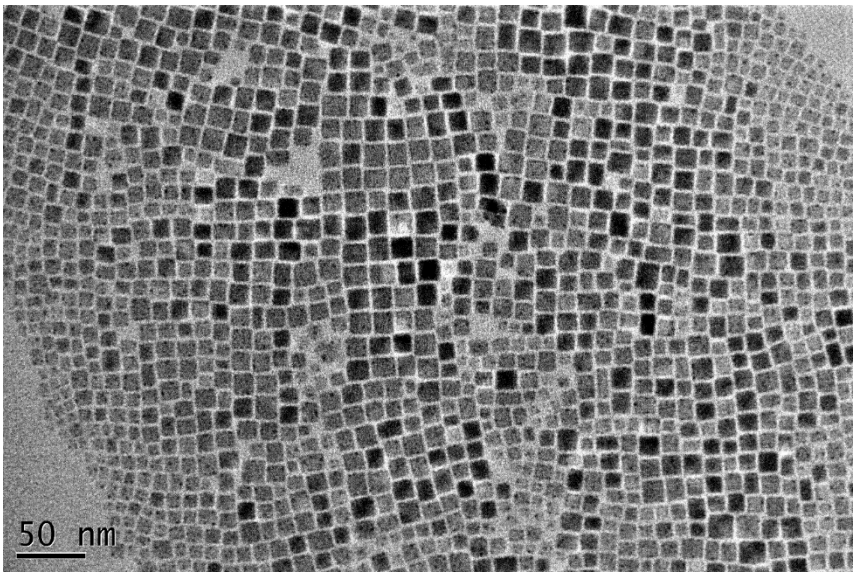

Figure 1. Transmission electron microscope image of standard $CsPbBr_3$ nanocrystals

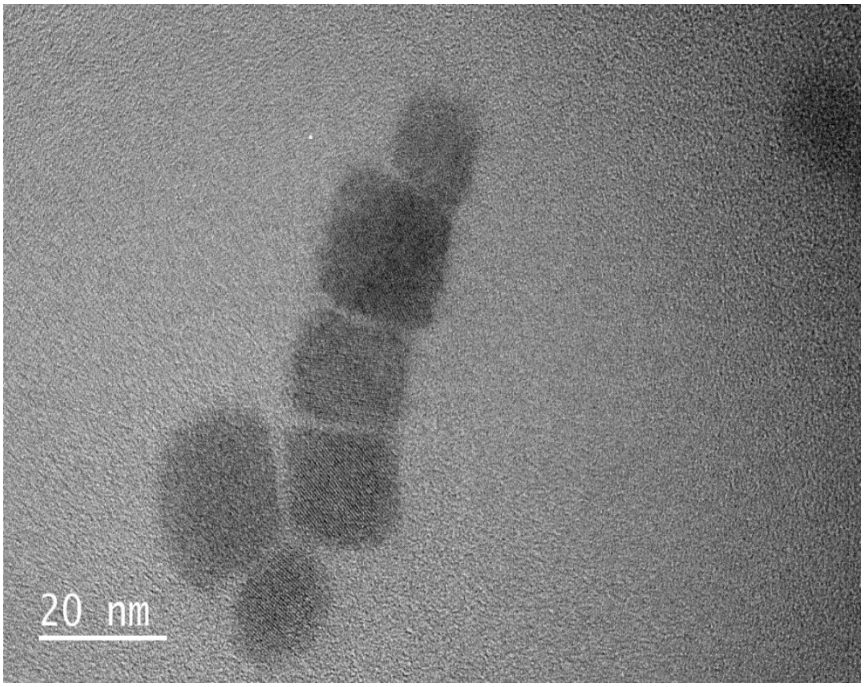

Figure 2. TEM image of $CsPbBr_3$ nanocrystals attached to SiO_2 nanoparticles of original diameter ~10 nm. Attachment is confirmed due to the optical absorption and PL matching standard solutions of $CsPbBr_3$ nanocrystals, while the TEM shows much larger sizes of the composite SiO_2/NC aggregates. There is insufficient contrast to distinguish the SiO_2 from the $CsPbBr_3$

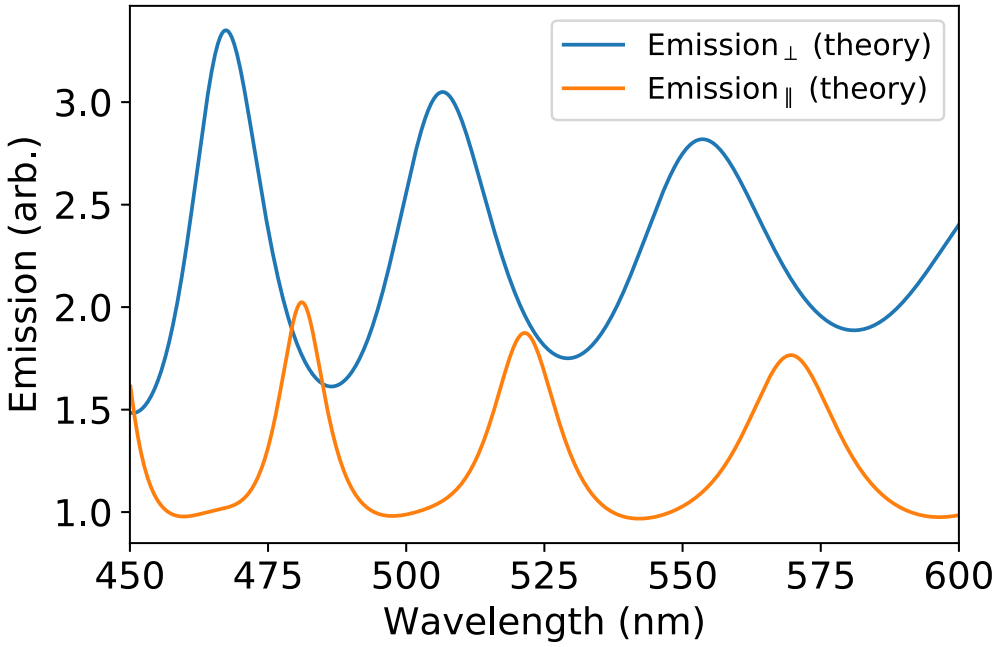

Figure 3. Simulated scattering modes of a 1.5 µm diameter SiO_2 microsphere, for a dipole perpendicular (blue line) to the coated sphere, and parallel (orange line). Simulations used publicly available codes (SPlaC)[1] implementing a generalization of Mie theory to dipolar emission near multilayer spheres.[2]

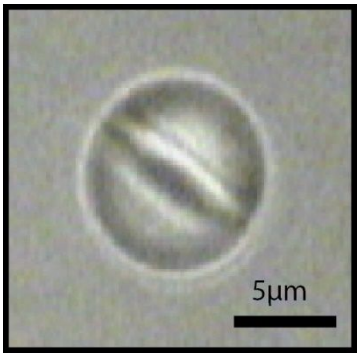

Figure 4. Optical microscopy image of an atypical SiO_2 microsphere with an apparent 'ring-like' coverage of perovskite nanoparticles.

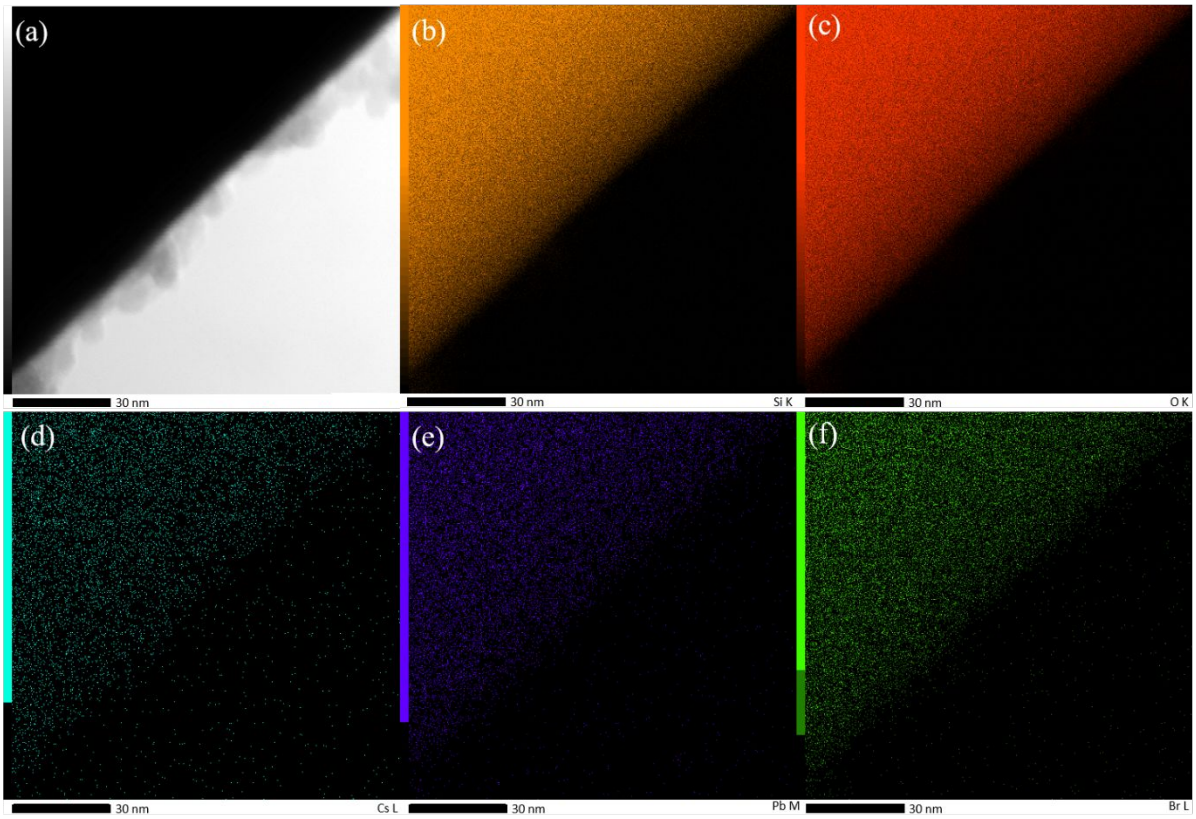

Figure 5. Elemental analysis of $CsPbBr_3$ nanocrystals attached to SiO_2 microparticles. (a) TEM image of $CsPbBr_3$ - SiO_2 microparticles. (b – f) elemental analysis maps: (b) Si, (c) O, (d) Cs, (e) Pb and (f) Br.

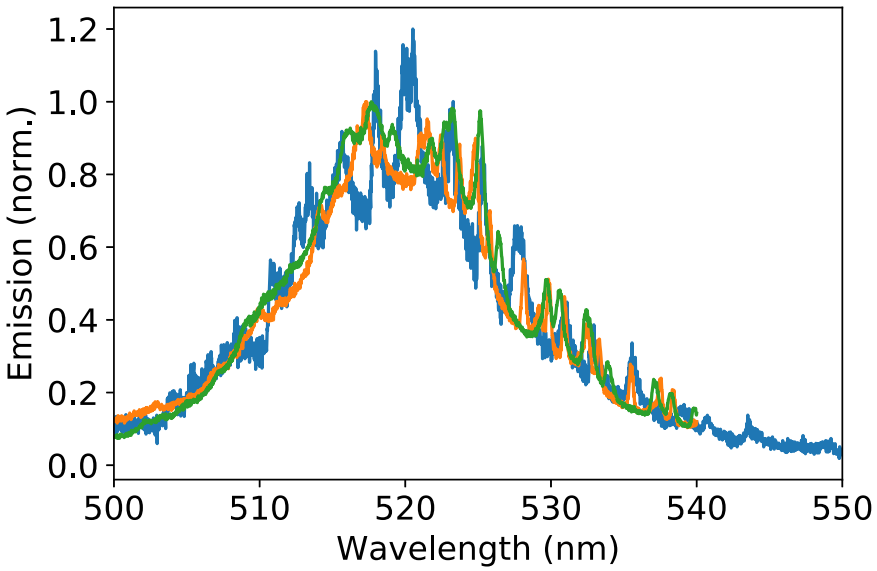

Figure 6. Emission from three different microspheres (green, blue and orange lines) measured individually using a joint photoluminescence and microscopy setup. The normalised emission

illustrates the smearing of the individual modes when the three emission curves are plotted on top of each other, but also illustrates substantial modal overlap at 527 nm where lasing from an ensembled was observed.

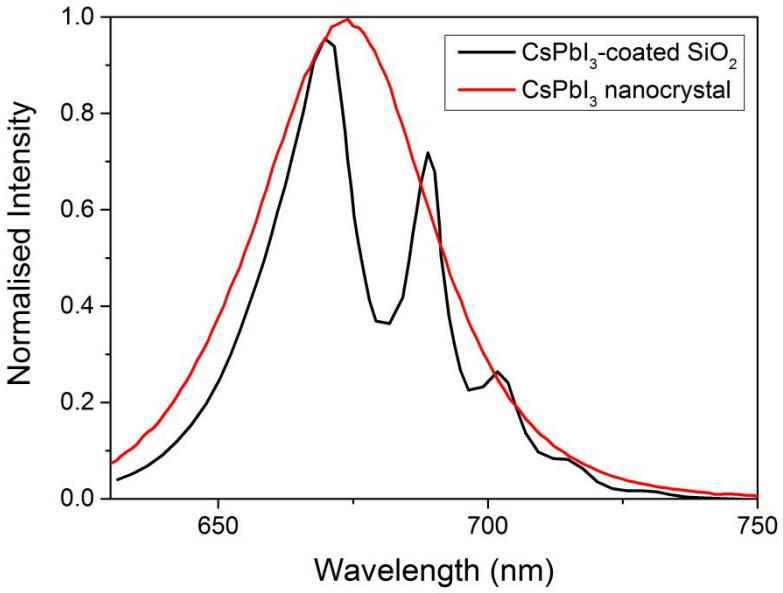

Figure 7. Whispering gallery mode emission in an individual $CsPbI_3$-coated SiO_2 microsphere (black line), measured under a photoluminescence microscope (excitation wavelength 458 nm). Emission of $CsPbI_3$ nanocrystals in solution, unattached to SiO_2, is overlaid (in red) for comparison.

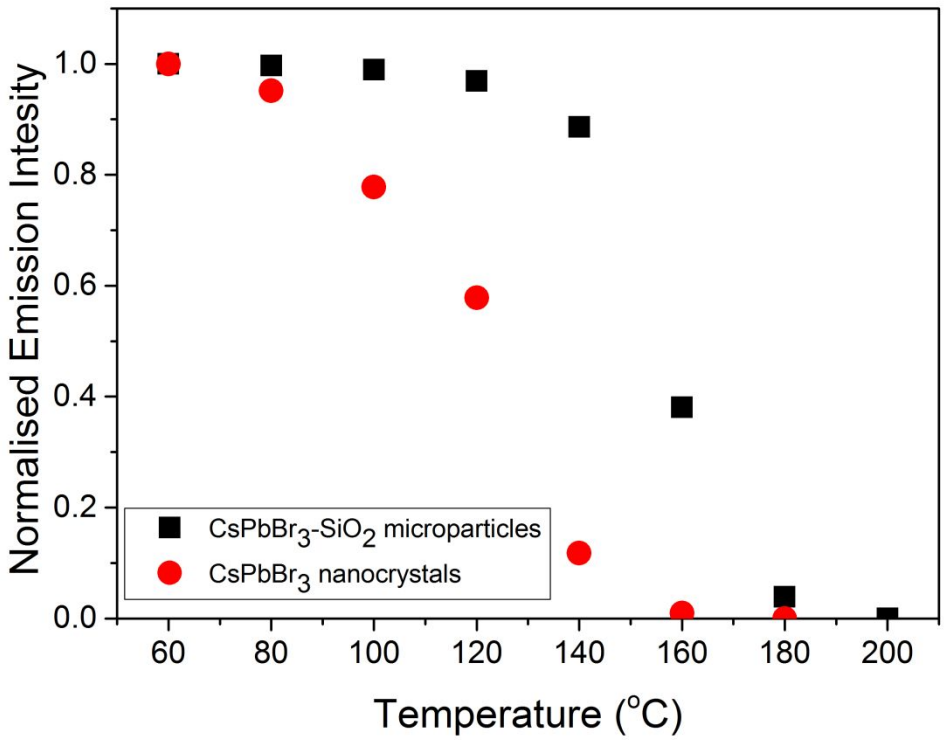

Figure 8. Thermal degradation of luminescence experiment of as is (red) and attached to SiO_2 (black) samples.

References:

(1) Le Ru, E. C.; Etchegoin, P., G. SERS and Plasmonics Codes (SPlaC), Matlab codes freely available from http://www.vuw.ac.nz/raman/book/codes.aspx.

(2) Le Ru, E., C.; Etchegoin P., G. *Surface Enhanced Raman Spectroscopy and Related Plasmonic Effects*; Elsevier: Amsterdam, 2009.